Electronic Supplementary Material (ESI) for Chemical Science.
This journal is © The Royal Society of Chemistry 2019

SUPPORTING INFORMATION

Peptide-Induced Super-Assembly of Biocatalytic Metal-Organic Frameworks for Programmed Enzyme Cascade

Jieying Liang,[a,b] Federico Mazur,[a] Chuyang Tang,[a] Xunan Ning,*[b] Rona Chandrawati*[a] and Kang Liang*[a,c]

[a]School of Chemical Engineering, The University of New South Wales, Sydney, NSW 2052, Australia
[b]School of Environmental Science and Engineering, Guangdong University of Technology, Guangzhou 510006, China
[c]Graduate School of Biomedical Engineering, The University of New South Wales, Sydney, NSW 2052, Australia

*E-mails: ningxunan666@126.com (X.N); rona.chandrawati@unsw.edu.au (R.C); kang.liang@unsw.edu.au (K.L)

***Materials*:** a-D-Glucose was purchased from Ajax Finechem; 2,2'-Azino-bis(3-ethylbenzothiazoline-6-sulfonic acid) diammonium salt (ABTS) was purchased from Roche (Australia); Glucose oxidase (GOx) was purchased from *Aspergillus niger*; Horseradish peroxidase (HRP), β-galactosidase (β-Gal), 3-amino-1,2,4-triazole (Atz), phosphate buffer saline (PBS, 1x), 2-methylimidazole, zinc nitrate hexahydrate (98%), protease from *Bacillus licheniformis* (2.4 U/g), Bradford reagent, 3-(*N*-Morpholino)propanesulfonic acid (MOPS) and tris(2-carboxyethyl)phosphine hydrochloride (TCEP) were purchased from Sigma-Aldrich (Australia). The polypeptides JR2KC (NAADLKKAIKALKKHLKAKGPCDAAQLKKQLKQAFKAFKRAG) and JR2EC (NAADLEKAIEALEKHLEAKGPCDAAQLEKQLEQAFEAFERAG) were purchased from Genscript (USA), with Mw 4584.5 and 86.2% purity for JR2EC and Mw 4577.2 and 90.5% purity for JR2KC. Succinimidyl-[(*N*-maleimidopropionamido)-diethyleneglycol] ester) (SM(PEG_2)) was purchased from Thermo Scientific (Australia). All reagents were used without further purification.

Supporting Discussion

Table S1 pH change during enzyme/ZIF-8 synthesis.

Enzyme	DI water	HmIm+Zinc nitrate	Reaction for 30 min	After 3 cycle centrifugations
GOx	6.63±0.02	9.58±0.02	9.57±0.02	8.77±0.02
HRP	7.07±0.02	9.59±0.02	9.55±0.02	8.64±0.02
β-Gal	4.53±0.02	9.55±0.02	9.55±0.02	8.79±0.02

Table S2 Percentage approximation of super-assembled enzyme/ZIF-8A structures in a given sample obtained via confocal microscopy.

Two-enzyme system	
GOx/ZIF-8A+HRP/ZIF-8A	45%
GOx/ZIF-8A+HRP/ZIF-8A+GOx/ZIF-8A	20%
HRP/ZIF-8A+GOx/ZIF-8A+HRP/ZIF-8A	23%
Others	12%
Three-enzyme system	
GOx/ZIF-8A+HRP/ZIF-8A	20%
β-Gal/ZIF-8A+GOx/ZIF-8A	18%
β-Gal/ZIF-8A+GOx/ZIF-8A+HRP/ZIF-8A	21%
β-Gal/ZIF-8A+GOx/ZIF-8A+β-Gal/ZIF-8A	17%
HRP/ZIF-8A+GOx/ZIF-8A+HRP/ZIF-8A	14%
Others	10%

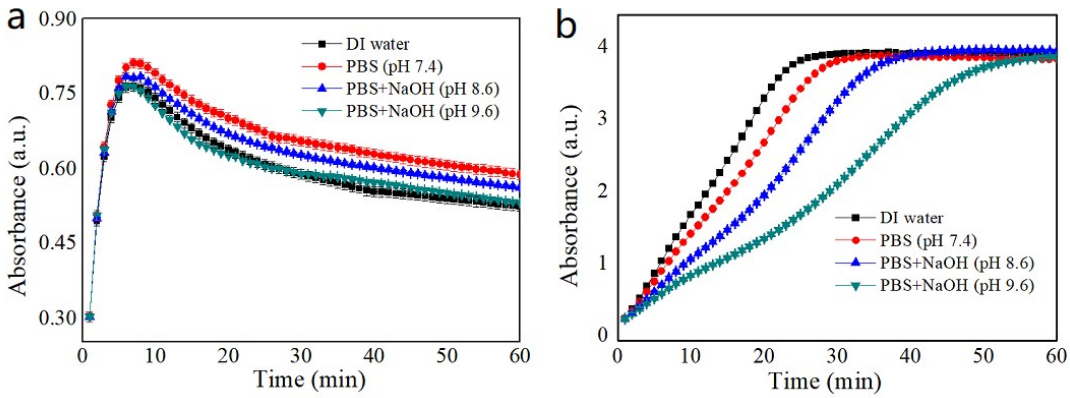

Fig. S1 Activity of enzymes in (a) the two-enzyme system and (b) three-enzyme system at the different pH conditions experienced during enzyme/ZIF-8A formation.

The pH of the enzymes suspended in DI water ranged from 4.53 to 7.07. After the addition of HmIm and Zinc nitrate, the pH increased to a final value of 8.64-8.79 for enzyme/ZIF-8A. For the two-enzyme system, 5 μg/ml free GOx and 5 μg/ml free HRP was added to a PBS solution containing 314 mM ABTS and 1.2 mM glucose. For the three-enzyme system, 5 μg/ml free GOx, 5 μg/ml free HRP and 5 μg/ml free β-Gal was added to a PBS solution containing 532 mM mM ABTS and 29 mM lactose. 1 M NaOH solution was used to adjust the pH.

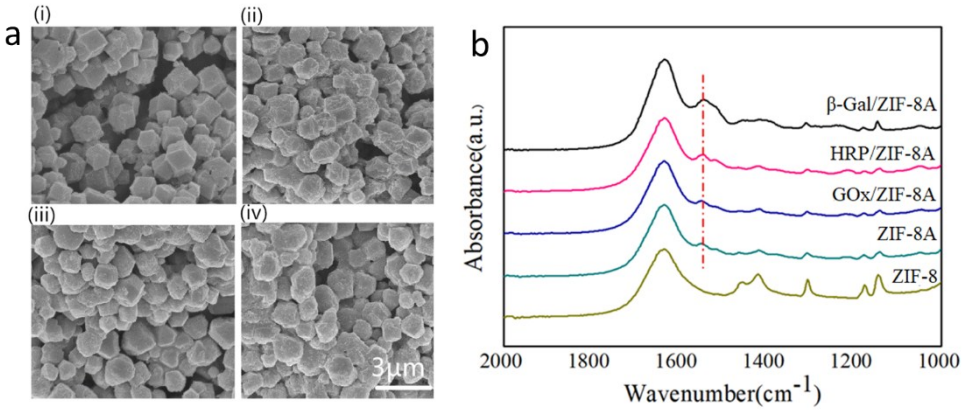

Fig. S2 Characterization of ZIF-8 and enzyme/ZIF-8: (a) SEM images of pure ZIF-8 (i); GOx/ZIF-8 (ii); HRP/ZIF-8 (iii); β-Gal/ZIF-8 (iv); (b) FTIR analysis of ZIF-8, ZIF-8A and enzyme/ZIF-8A.

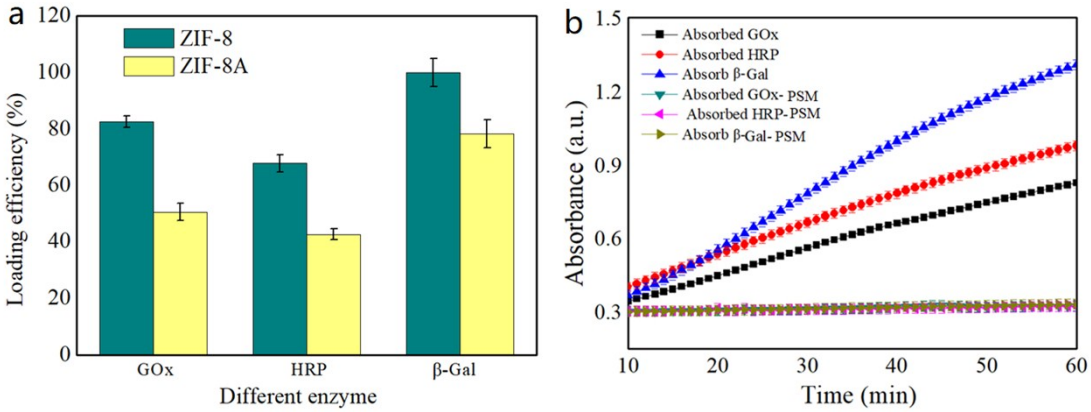

Fig. S3 (a) Enzyme loading efficiency in ZIF-8 and ZIF-8A, determined by the fluorescently labelled proteins method. (b) Presence of enzyme on the ZIF-8 surface and removal of enzyme after PSM process.

Fig. S3a shows the enzyme loading efficiency of GOx, HRP and β-Gal in ZIF-8 was calculated to be 82.0%±2.0%, 67.8%±3.2% and 101.1%±5.2% using the fluorescently labeled protein method. However, after carrying out the PSM method for amine-fountionalization, the enzyme loading efficiency of GOx, HRP and β-Gal in ZIF-8 was 50.6%±2.0%, 42.7%±2.2% and 78.3%±4.2%. The results suggest enzymes present in the peripheral region of the MOFs are removed during the PSM process. This could be due to the weak non-covalent interactions between enzymes and ZIF-8. A particle tracking analysis (NanoSight NS300) was carried out to quantify the number of enzymes encapsulated within the MOF. Using this method, this is $(1.8\pm1.2)\times10^5$ particles per μL. Therefore, the amount (mg) of enzymes encapsulated in GOx/ZIF-8A, HRP/ZIF-8A and β-Gal/ZIF-8A was caculated as $(2.6\pm1.8)\times10^{-5}$, $(2.2\pm1.5)\times10^{-5}$, and $(4\pm2.8)\times10^{-5}$ mg per ZIF-8A particle, respectively.

In Fig. S3b, 60 μg/ml GOx/ZIF-8A was mixed with 5 μg/ml free HRP, 60 μg/ml HRP/ZIF-8A was mixed with 5 μg/ml free GOx, 60 μg/ml GOx/ZIF-8A and 60 μg/ml HRP/ZIF-8A were mixed with 5 μg/ml free β-Gal. After 3 washing cycles, the resulting enzyme/ZIF-8A showed cascade activity, implying that GOx, HRP and β-Gal were present on the surface of ZIF-8A. However, after incubation at 50 °C for 2 h, the enzyme/ZIF-8 did not show cascade activity, suggesting the enzyme on the surface of ZIF-8A was removed or denatured during the PSM process for amine group functionalization on enzyme/ZIF-8.

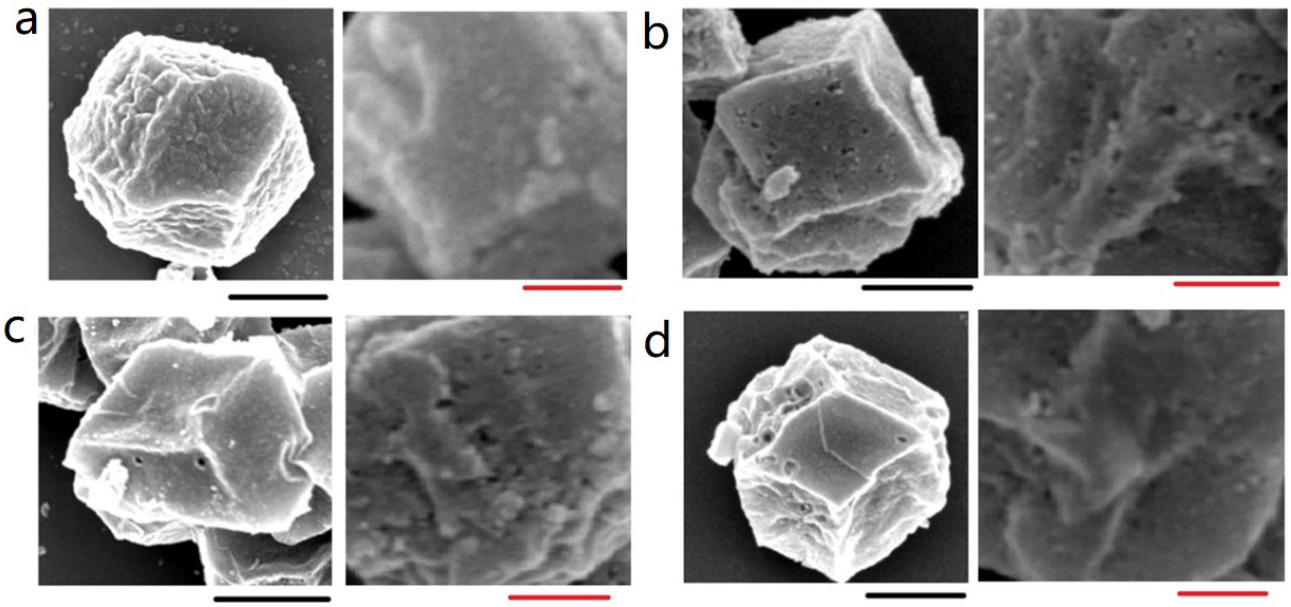

Fig. S4 The surface of enzyme/ZIF-8A (left, scale bar 300 nm) and their cross-sectional SEM image (right, scale bar 100 nm) after calcination treatment at 325 °C for 30 min in air. (a) pure ZIF-8A; (b) GOx/ZIF-8A; (c) HRP/ZIF-8A; (d)β-Gal/ZIF-8A.

The aperture size of ZIF-8 (3.4 Å) is smaller than glucose (8.4 Å), lactose (11.8 Å) or ABTS (10.1 × 17.3 Å).[1,2] However, previous studies have shown that the framework of ZIF-8 is flexible, which could allow the passage of larger molecules.[2] In addition, by introducing enzymes in the crystal lattice of ZIF-8, large defects from the crystals are introduced, as reported in our and other groups' studies.[3-6] As seem from Fig. S4, after the calcination treatment at 325 °C for 30 min in air, enzyme molecules were removed from the ZIF-8A by leaving a void structure where the enzyme was originally located (Figure S4), while no such void structure was presented in the interior of pure ZIF-8A after the same calcination treatment. The defect or the voids on the surface and in the interior of ZIF-8A would allow the subtracts to flow into the ZIF-8A and react with enzyme inside the ZIF-8A. Furthermore, control experiments proved that no enzymes were attached to the surface of enzyme/ZIF-8A (Fig. S3) and excluded other possible catalytic mechanisms (See Fig. S3, S6, S12). These results and previous works[7,8] confirmed the enzyme cascade reactions were induced by the enzymes inside the MOFs.

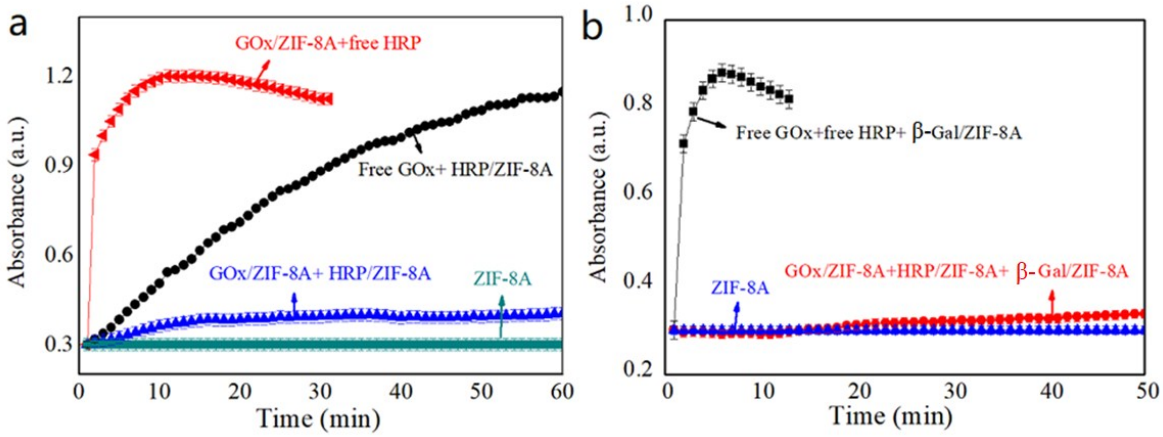

Fig. S5 (a) Time-dependent absorbance changes observed by a two-enzyme cascade reaction (220 μL solution contains 314 mM ABTS, 1.2 mM glucose, 60 μg/ml GOx/ZIF-8A, 60 μg/ml HRP/ZIF-8A, or 5 μg/ml free enzymes); (b) Time-dependent absorbance changes observed by a three-enzyme cascade reaction (270 μL solution contains 532 mM ABTS, 29 mM lactose, 60 μg/ml GOx/ZIF-8A, 60 μg/ml HRP/ZIF-8A, 60 μg/ml β-Gal/ZIF-8A, or 5 μg/ml free enzymes).

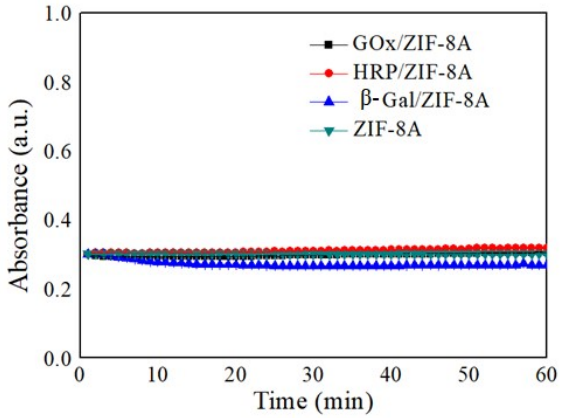

Fig. S6 Activity of single enzyme/MOF. The activity of 60 μg/ml GOx/ZIF-8A, 60 μg/ml HRP/ZIF-8A, or 60 μg/ml β-Gal/ZIF-8A in the reaction mixture (314 mM ABTS and 1.2 mM glucose for two enzyme system and 532 mM ABTS and 29 mM lactose for three-enzyme system).

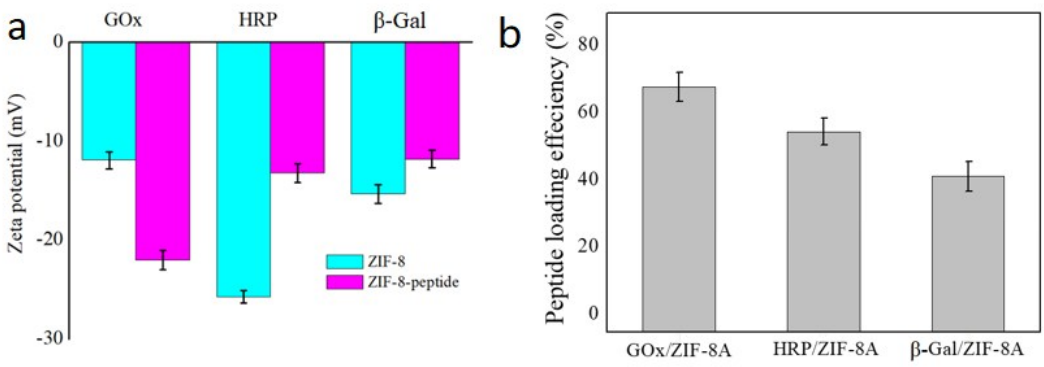

Fig. S7 (a) Zeta potential of enzyme/ZIF-8 and their peptide conjugates. JR2EC conjugated to GOx/ZIF-8A, JR2KC conjugated to HRP/ZIF-8A and β-Gal/ZIF-8A. (b) Determination of the peptide loading efficiency on the enzyme/ZIF-8A via Braford assay.

The concentrations of unbound peptides in the supernatant were determined via Braford assay method. The conjugation efficiency of peptides on the GOx/ZIF-8A, HRP/ZIF-8A and β-Gal/ZIF-8A was calcualted to be 68.0%±4.3%, 54.7%±4.0% and 41.3%±4.5%, respectively.

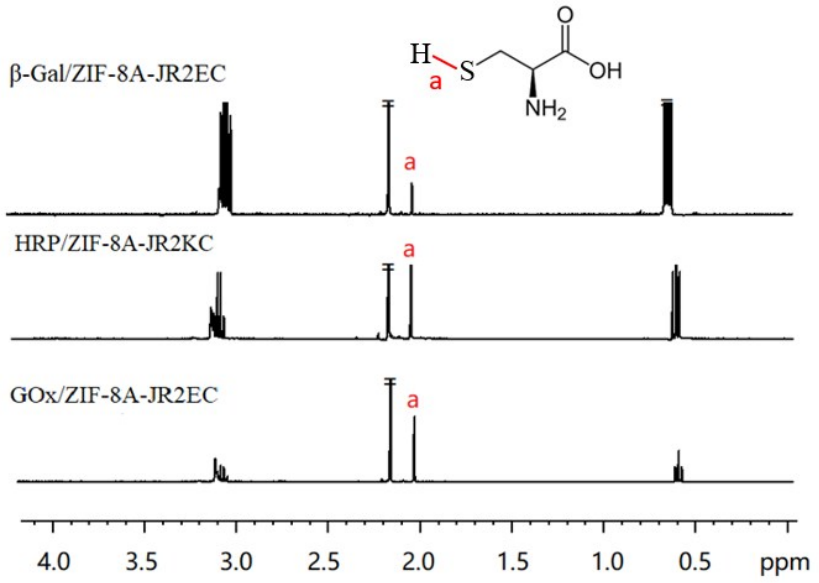

Fig. S8 ^{1}H NMR spectra of JR2EC-functionalized GOx/ZIF-8A, JR2KC-functionalized HRP/ZIF-8A and JR2KC-functionalized β-Gal/ZIF-8A.

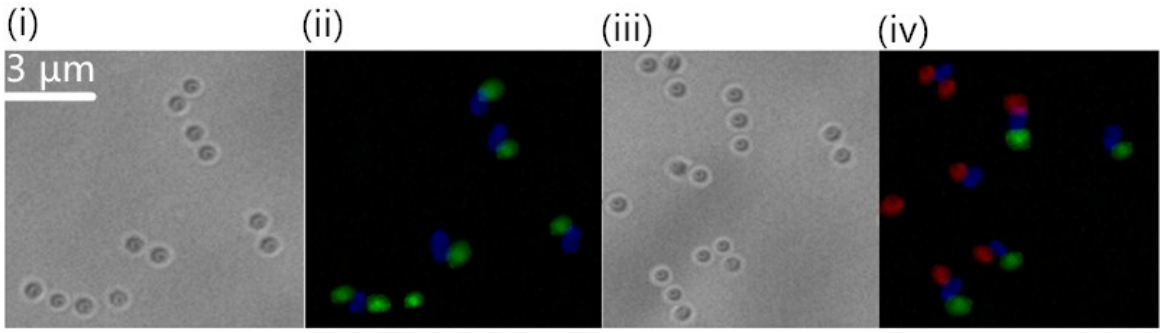

Fig. S9 Confocal microscopy of the super-assembled enzyme/ZIF-8A structures via JR2EC/JR2KC coiled-coil formation. (i) Bright-field images of the super-assembled GOx/ZIF-8A and HRP/ZIF-8A and (ii) their confocal images. (iii) Bright-field images of the super-assembled GOx/ZIF-8A, HRP/ZIF-8A, and β-Gal/ZIF-8A and (iv) their confocal images. GOx was labeled with Alexa Fluor 350 NHS ester (blue); HRP was labeled with FITC (green); β-Gal was labeled with Atto 647N NHS ester (red).

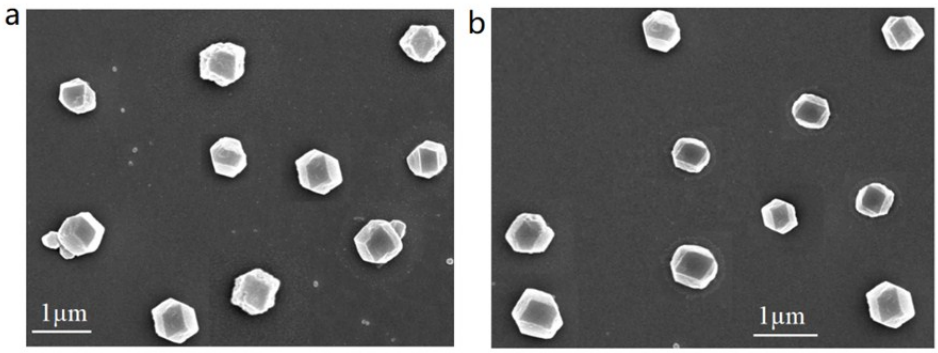

Fig. S10 SEM images of (a) JR2EC-founctionalized GOx/ZIF-8A only and (b) a mixture of JR2KC-founctionalized HRP/ZIF-8A and JR2KC-founctionalized β-Gal/ZIF-8A.

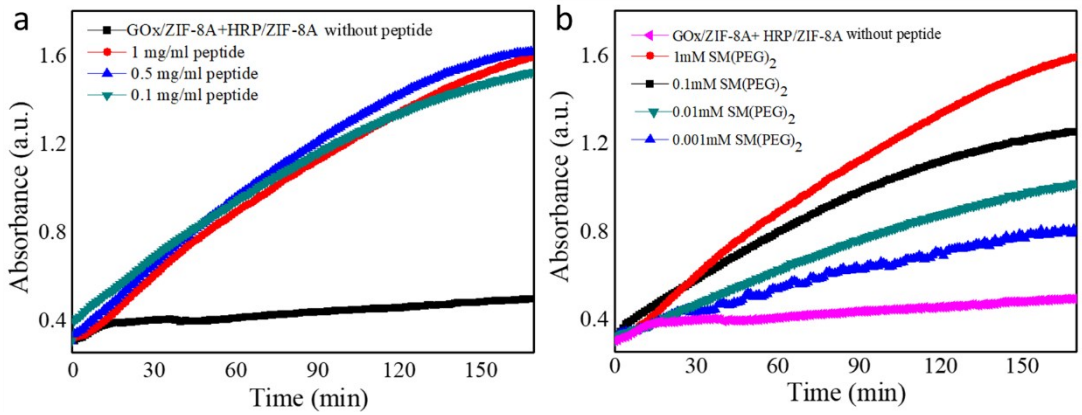

Fig. S11 Effect of peptide and crosslinker ($SM(PEG)_2$) concentration on the cascade reaction of glucose when mixing GOx/ZIF-8A and HRP/ZIF-8A. (a) Different concentrations of peptide (0.1, 0.5 and 1 mg/mL) and 1mM crosslinker ($SM(PEG)_2$). (b) Different concentration of ($SM(PEG)_2$ (0.001, 0.01, 0.1 and 1 mM) and 0.1 mg/ml peptide.

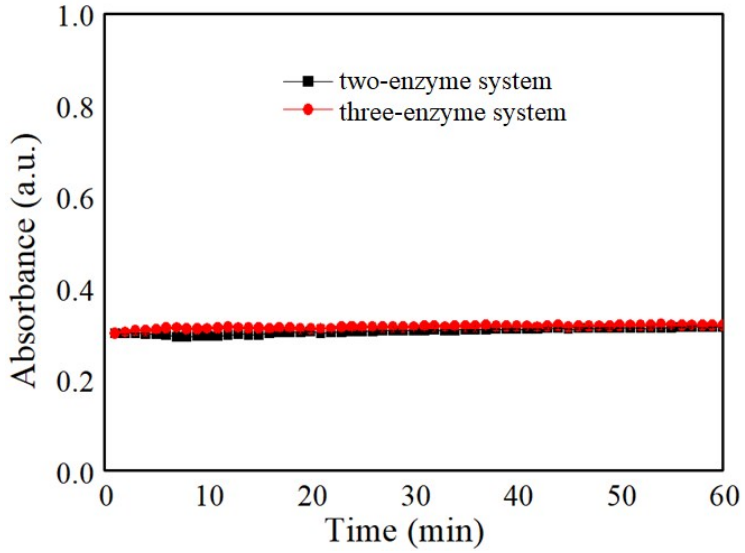

Fig. S12 Control experiment of peptide functionalized ZIF-8A without enzyme. For the two-enzyme system, 60 μg/ml ZIF-8A-JR2EC and 60 μg/ml ZIF-8A-JR2KC were mixed in a PBS solution containing 314 mM ABTS and 1.2 mM glucose. For the three-enzyme system, 60 μg/ml ZIF-8A-JR2EC, 60 μg/ml ZIF-8A-JR2KC and 60 μg/ml ZIF-8A-JR2KC were added in a PBS solution containing 532 mM ABTS and 29 mM lactose.

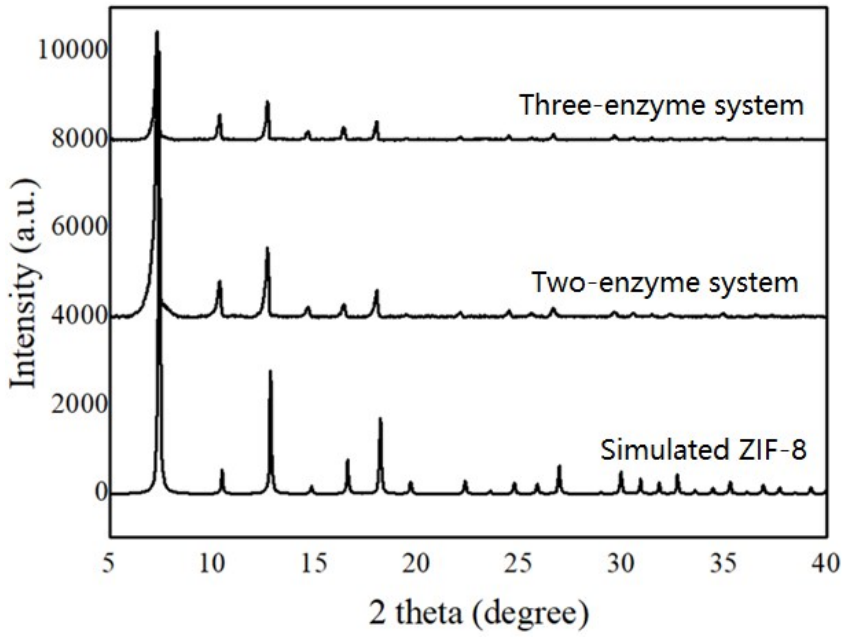

Fig. S13 PXRD patterns for the two-enzyme system (GOx/ZIF-8A and HRP/ZIF-8A) composites and three-enzyme system (GOx/ZIF-8A, HRP/ZIF-8A and β-Gal/ZIF-8A) composites after the biocatalytic reactions.

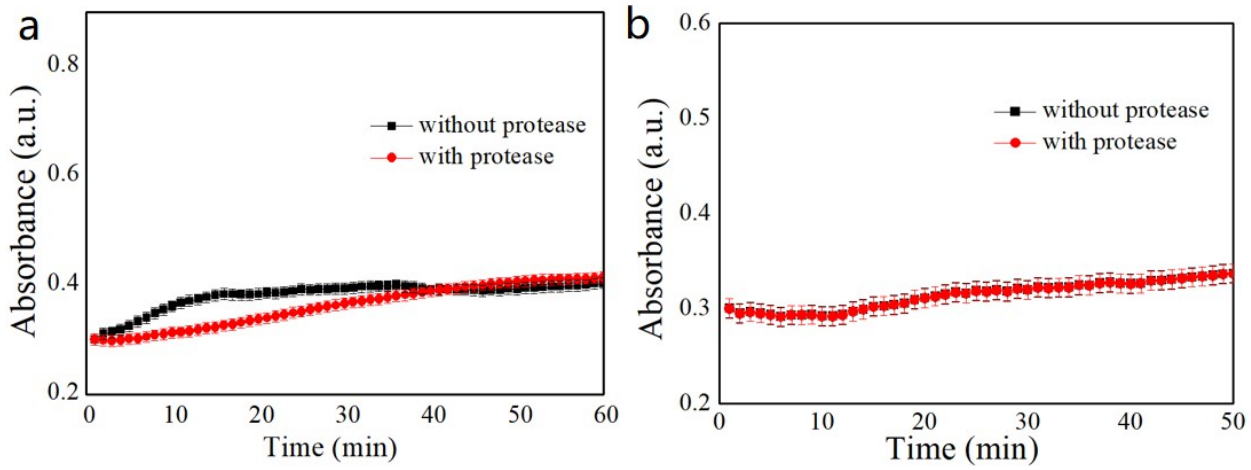

Fig. S14 The activity of the enzyme/ZIF-8A particles without peptides against protease digestion in (a) two enzyme/ZIF-8A system and (b) three enzyme/ZIF-8A system.

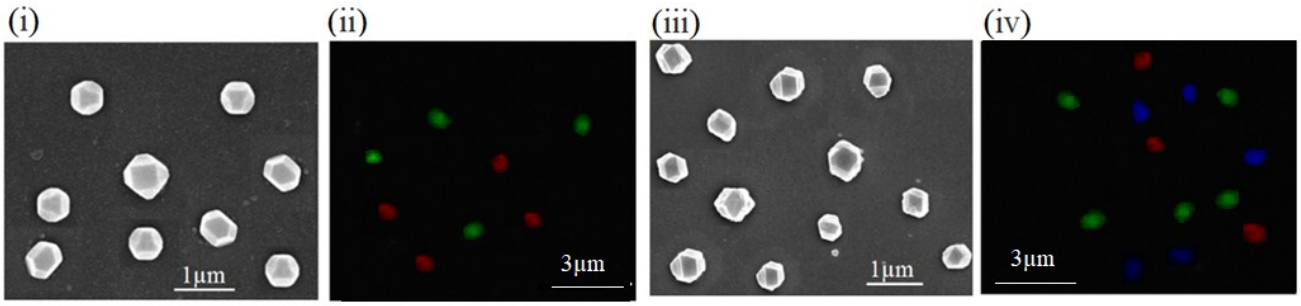

Fig. S15 SEM and confocal microscopy images after the addition of protease into the super-assembled two enzyme/ZIF-8A system (i, ii) and three enzyme/ZIF-8A system (iii, iv).

References:

1 Y. Chen, V. Lykourinou. T, Hoang, L. J. Ming and S. Ma. *Inorg. Chem.* 2012, **51**, 9156-9158.
2 C. Zhang, Ryan P. Lively, K. Zhang, Justin. R. Johnson, O. Karvan and W. J. Koros. *J. Phys. Chem. Lett.* 2012, **3**, 2130-2134.
3 K. Liang, R. Ricco, C. M. Doherty, M. J. Styles, S. Bell, N. Kirby, S. Mudie, D. Haylock, A. J. Hill, C.J. Doonan and P. Falcaro, *Nat. Commun.*, 2015, **6**, 7240.
4 K. Liang, J. J. Richardson, C. J. Doonan, X. Mulet, Y. Ju, J. Cui, F. Caruso and P. Falcaro, *Angew. Chem. Int. Ed.* 2017, **56**, 8510-8515.
5 K. Liang, C. J. Coghlan, S. G. Bell, C. Doonan and P. Falcaro, *Chem. Commun.* 2016, 52, 473-476.
6 F. Lyu, Y. Zhang, R.N. Zare, J. Ge and Z. Liu, *Nano Lett.* 2014, 14, 5761-5765.
7 W. H. Chen, M. Vázquez-González, A. Zoabi, R. Abu-Reziq and I. Willner, *Nat. Catal*. 2018, **1**, 689-695.
8 X. Wu, J. Ge, C. Yang, M. Hou and Z. J. C. C. Liu, *Chem. Commun*., 2015, **51**, 13408-13411.